Euro-Mediterr J Environ Integr (2017) 2:19
DOI 10.1007/s41207-017-0030-0

ORIGINAL PAPER

Simultaneous adsorption behavior of heavy metals onto microporous olive stones activated carbon: analysis of metal interactions

Thouraya Bohli[1] · Abdelmottaleb Ouederni[1] · Isabel Villaescusa[2]

Received: 31 January 2017 / Accepted: 25 July 2017 / Published online: 8 August 2017

Abstract The present work reports the synergistic and inhibitory adsorption effects involved in the multicomponent adsorption of heavy metal ions (Cu(II), Ni(II), and Cd(II)) from binary systems using chemically olive stone activated carbon (COSAC) as adsorbent. In order to evaluate the adsorption capacity of COSAC to remove studied heavy metals, adsorption of metal ions in single and binary systems were conducted. Kinetics adsorption rates in binary systems are very fast as compared to that in single ones and well represented by the pseudo second-order. Langmuir and Sips model fit mono-solute adsorption isotherms and the maximum adsorption capacity of COSAC decreased in the following order: Cd(II) > Ni(II) > Cu(II). In binary equilibrium systems, the effect of initial concentration of interfering metal ions on the removal of target ones was studied. Different mutual interactions between metal ions dealing with the decrease and the enhancement of inhibitory and synergetic effects were detected. Results showed that the effects on the adsorption of the metal ions in binary mixture strongly depend on the initial concentration of both metal ions in the solution. In most of the scenarios studied, the total amount of metal ions adsorbed was higher than the sum of the ones obtained in single solutions, suggesting synergetic interactions between the two metal ions. This study proves that COSAC is an effective adsorbent for the removal of heavy metals from multicomponent solutions.

Keywords Activated carbon · Heavy metals · Complex adsorption · Metals interactions

✉ Thouraya Bohli
bohlithouraya@gmail.com

[1] Laboratory of Research: Process Engineering and Industrial Systems (LR11ES54), National School of Engineers of Gabes, University of Gabes, 6026, Gabes, Tunisia

[2] Department d'Enginyeria Quimica, Agraria i Tecnologia Agroalimentaria, Universitat de Girona, Ma Aurèlia Capmany, 17003 Girona, Spain

Introduction

Heavy metal discharges from different industries cause surface and underground water pollution. Heavy metals, such as Cu(II), Ni(II), and Cd(II) are toxic to human beings and other living organisms even at diluted concentrations (Ahmad et al. 2010; Laus and de Favere 2011; Cui et al. 2016). Because heavy metals are hazardous, it is necessary to regulate their levels in water intended for human consumption, as well as in industrial effluents. Therefore, the World Health Organization (WHO 2011) and Tunisian authorities (NT 1989) have given recommendations that take into account risk and fix maximum permissible concentrations of heavy metals in wastewaters and drinking water. To get concentrations under the maximum allowable values of heavy metals in effluents and industrial wastewaters, several works were focused on developing effective and new technologies adequate to reduce the concentration or to change the physico-chemical properties of these pollutants.

Adsorption by porous solids, as activated carbons, is considered as an effective process for heavy metal removal thanks to its simplicity, low cost, environmental friendliness, processing with no chemical sludge, and high removal efficiency even at diluted concentration (Porpuri et al. 2009; Cui et al. 2016). The use of agriculture by-products such as coconut fruit (Anirudhan and Sreekumari 2011), nuts apricot (Tsibranska and Hristova 2010), beet

pulp (Pehlivan et al. 2008), stems of tea (Amarasinghe and Williams 2007), rice husk (Bakircioglu et al. 2003; Wong et al. 2003), pentandra hulls (Madhava-Raoa et al. 2006)and olive stones-waste (Alslaibi et al. 2015; Baccar et al. 2009; Gharib and Ouederni 2005), which are inexpensive, abundantly available, and renewable materials, as precursor for activated carbon production, reduces adsorption processing costs (Bailey et al. 1999). The adsorption process offers flexibility in design and operation and in many cases will produce high-quality treated effluent (Fu and Wang 2011; Cui et al. 2016). Moreover, because adsorption is usually reversible, adsorbents can be regenerated via suitable desorption processes.

Activated carbon (AC) was mainly used as effective adsorbent of heavy metals removal thanks to its highly developed pore structure and large surface area (Knaebel 1995). Diverse acidic and basic surface functional groups in AC, especially oxygen-containing groups (carboxylic, phenol, lactone), which are mostly hydrophilic in nature, can easily adsorb the polar species from the solution (Brasquet et al. 2002; Li et al. 2003; Singha et al. 2013; Zhang et al. 2015). The last cited authors reported that an activated carbon with a high amount of carboxylic groups and low pH_{pzc} is an effective adsorbent of heavy metals. The diverse characteristics of activated carbon are incorporated by physical or chemical activation and depend on the type of precursor, activation conditions, activation agent, and mode (Kasnejad et al. 2012; Ceyhan et al. 2013). Furthermore, the non-uniform adsorption sites in AC provide complex and varied interactions during the adsorption process (Luo et al. 2015).

Adsorption of various heavy metals from single metal solutions has been extensively investigated (Gao et al. 2009; Abbas et al. 2013; Bohli et al. 2015; Depci et al. 2012). However, only few publications are devoted to the studies of simultaneous adsorption of metal ions from aqueous solutions (Luo et al. 2015; Ma et al. 2015). This is a direct consequence of the difficulty of experimentation and analysis involved in multicomponent adsorption studies, but it is a fact that natural water or wastewater effluents often contain more than one heavy metal, which can potentially modify the type of interactions (additive, synergetic, and antagonistic) between metal ions that result in a competition for AC adsorption sites. Thus, it is important to understand the details about these interactions to better understand the exact adsorption mechanism of heavy metal adsorption onto activated carbon produced from olive stones (COSAC) in multicomponent systems. Unfortunately, the majority of researchers studying multi-components adsorption processes focus on modeling adsorption data without undertaking any discussions about the interaction mechanisms that can take place.

In this work, adsorption of Cu(II), Ni(II), and Cd(II) in single and binary systems onto an olive stones chemically activated carbon (COSAC) has been studied. The analysis interactions between metal ions in binary mixtures for binding adsorbent active sites were investigated by plotting isotherms of target metal containing varying initial concentration of interfering metal.

Materials and methods

Chemicals

Copper nitrate (99.5%), cadmium nitrate (99%), and nickel nitrate (98%) used in this study were of analytical grade. Heavy metal stock solutions of 10 mmol/l were prepared by dissolving required amounts of $Cu(NO_3)_3{\cdot}H_2O$, $Ni(NO_3)_2{\cdot}6H_2O$ and $Cd(NO_3)_2{\cdot}4H_2O$ salts in double-distilled water. Lower metal concentrations were obtained by simple dilution.

Activated carbon preparations

The activated carbon used in this work was prepared from olive stone according to an optimized protocol (Bohli et al. 2015; Gharib and Ouederni 2005): crude olive stones were impregnated with a phosphoric acid solution (50% by weight) at 110 °C in a flask fitted with a reflux condenser for 9 h. After drying, the impregnated material was subjected to thermal activation, 170 °C for 30 min and then 410 °C for 150 min, in a vertical tubular reactor fed by a stream of nitrogen. The activated carbon obtained, labeled as COSAC, was washed thoroughly with distilled water to eliminate impurities, dried at 60 °C for 24 h, and then sieved.

The main chemical and physical characteristics of the used activated carbon (COSAC) were presented in detail in our previous works (Bohli and Ouederni 2016; Bohli et al. 2015). Total surface area was determined using the Brunauer–Emmett–Teller (BET) equation. The elemental composition of COSAC surface was determined using XPS technique. The point of zero charge was determined via batch equilibrium technique (Slobodan et al. 2007). Surface functional groups were determined by the known Boehm titration (Wibowo et al. 2007).

Adsorption isotherms

Batch equilibrium adsorption experiments in monosolute and binary systems were conducted in isothermal conditions at 30 ± 1 °C. Fixed weight of chemically olive stone activated carbon samples of 0.3 g, with average particle size of 0.375 mm, were placed into a series of 250-ml Erlenmeyer flasks containing 50 ml of metal solution. To

obtain binary mixtures isotherms initial concentration of target metal ion was varied from 0.5 to 5.0 mmol/l while the initial concentration of the interfering metal ion was fixed to 0–0.5–1.0–2.0–3.0–4.0 and 5.0 mmol/l, respectively for each isotherm. Referring to a pH-effect study in previous work (Bohli et al. 2015), for all solutions the initial pH was fixed at 5.0 to avoid precipitation. The flasks were placed on a temperature-controlled multi-position magnetic shaker and shaken at 400 rpm for 10 h. This equilibrium contact time was optimized in a previous work (Bohli et al. 2015). Then, after filtration through a 0.45-µm cellulose filter paper, metal solutions were diluted with nitric acid (5% by weight) to be ready for analysis by ICP-AES spectrometry.

Kinetic studies of Cu(II), Ni(II), and Cd(II) were also performed in mono and binary systems solutions via batch mode in the same conditions. A volume of 500 ml of metal ion solution with initial concentrations of 1 mmol/l was poured into a jacketed reactor vessel maintained under a fixed stirring speed of 300 rpm. When the desired value (30 ± 1 °C) of solution temperature was reached, using a thermostatic bath circulation, 3 g of a COSAC with selected granulomere was added. Samples of 2 ml were withdrawn at a pre-set time intervals, then directly filtered, diluted, and acidified to be ready for analyses.

The metal ion concentrations were determined by an inductively coupled plasma-atomic emission spectrometer (ICP-AES; Activa-M, HORIBA Jobin Yvon) at wavelengths of 324.754, 221.647, and 228.802 nm, respectively for Cu(II), Ni(II), and Cd(II).

Adsorption experiments were carried out in duplicate measurement and the average results are presented herein. The adsorption capacities of activated carbons were calculated at equilibrium by using the following equation:

$$q_e = \frac{(C_0 - C_e)V}{m}, \quad (1)$$

where q_e is the adsorption capacity (mmol/g), V is the volume of the solution (L), C_0 is the initial metal ion concentration (mmol/l), C_e is the equilibrium metal ion concentration (mmol/l), and m is the initial dry mass of the activated carbon (g).

Results and discussion

Activated carbon characteristics

The main important characteristics of COSAC are illustrated in Table 1. The adsorbent COSAC has a high specific surface area of 1280 m^2/g and a developed microporous structure. The volume of the micropores represents 98% of total pore volume.

Table 1 Properties of COSAC

Physical properties	Chemical properties
Total area (BET) 1280 m^2/g	Carboxylic groups 0.512 meq/g
Micropore volume 0.552 cm^3/g	Carbonyl groups 1.829 meq/g
Total pore volume 0.561 cm^3/g	Lactonic groups 0.405 meq/g
Average pore diameter 20.72 A°	Phenolic groups 0.835 meq/g
	Total basic groups 0.198 meq/g
	pH_{pzc} 3.40

The elemental surface composition of COSAC was determined using XPS technique. Figure 1 shows elements relative peaks detected in COSAC expressed in At %. COSAC contains mainly carbon (90.93%), oxygen (5.28%), low bore (2.58%), and phosphorus (1.21%). The presence of the small percentage of phosphors results from the use of phosphoric acid as activating agent.

Results of Boehm titration (Table 1) indicate that the acidic character of the adsorbent is due to the predominance of acidic functional groups such as: carbonyl, phenol, and carboxylic, whereas with a total acid functional group concentration of 3.581 meq/g whereas the total basic functional groups concentration is 0.198 meq/g.

The point of zero charge or the net surface charge, known as pH_{pzc}, describes the pH conditions when electrical global charge density on the surface of the adsorbent is zero. The pH_{pzc} value of COSAC was found to be 3.40 (Table 1) and confirms the acid character of COSAC.

Adsorption kinetic studies

The competitive kinetic adsorption of Cu(II), Ni(II), and Cd(II) in binary systems was carried out using pairs of metal ions at the same ratio 1:1 of initial concentrations in solution and compared to single ones. In order to analyze the adsorption kinetics of heavy metal ions in binary

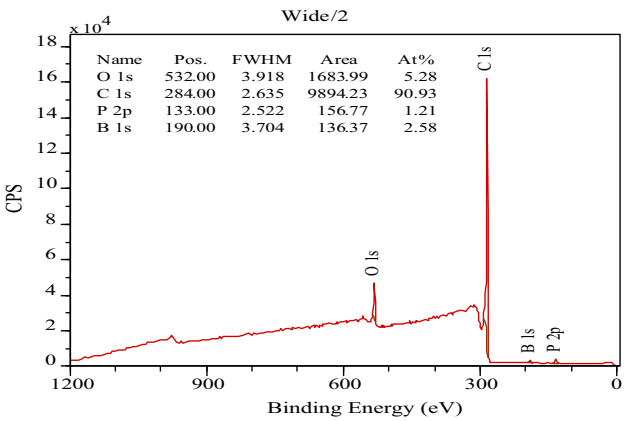

Fig. 1 XPS analysis of COSAC

systems, kinetic data were fitted to the pseudo-second-order model. The linear expression of the pseudo-second-order is given by the following equation:

$$\frac{t}{q_t} = \frac{1}{k_2 q_e^2} + \frac{1}{q_e} t, \quad (2)$$

where q_e and q_t are the adsorbed amounts of the solute (mmol/g or mg/g) at equilibrium and t time t (min) and k_2 is the pseudo-second-order rate constant (g/mmol min or g/mg min). Thereafter, the initial adsorption rate, defined as $h = k_2 q_e^2$, can be determined (mg/g min or mmol/g min).

The kinetic parameters resulting from fitting experiments, correlation coefficients, and calculated external mass transfer coefficient k_L (cm/s) are reported in Table 2. The external mass transfer coefficient was calculated using the following equation (Depci et al. 2012):

$$k_L = \frac{m k_2 q_e^2}{C_0 A}, \quad (3)$$

where m is the mass of adsorbent (g), k_2 is the pseudo-second-order rate constant (g/mmol min), q_e is the metal ions adsorbed (mmol/g), C_0 is the initial metal ion concentration (mmol/l), and A is the external surface area of adsorbent (m^2/g).

The kinetic adsorption behavior of Cu(II)–Ni(II), Cu(II)–Cd(II), and Cd(II)–Ni(II) binary systems are shown in Fig. 2. It can be seen that the individual uptake of these heavy metals were reduced in the binary component systems as compared to ones from single systems. This suggests that there is higher competition between ions coexisted in solutions.

During Cu(II)–Ni(II) adsorption process (Fig. 2a), Cu(II) uptake shows an increase as time progresses until reaching the equilibrium around 120 min, which was two times more rapid than single kinetic adsorption (240 min). It seems that copper with strong affinity to COSCA displaced a part of adsorbed nickel with lower affinity and takes its place. The adsorbed amount of Ni(II) was maintained more or less constant since the first contact times and achieved 0.015 mmol/g, 85% lower than the adsorbed amount of Ni(II) in single system. The experimental adsorbed amount of Cu(II) from the binary system was about 0.076 mmol/g, 15% lower than that in single system. The kinetic parameter h (mmol/g min) determined by the perfect fitting of experimental data to the pseudo-second-order for both Cu(II) and Ni(II) were 2.15 and 1.24, respectively. Thus, in binary, as in single systems, the kinetic adsorption order follows Cu(II) > Ni(II).

The kinetic curves of Cu(II) and Cd(II) in single and binary systems show similar shapes (Fig. 2b). Adsorption increases for both metals with contact time until equilibrium was reached at about 110 min for Cd(II) and 240 min for Cu(II). Like in the single solution, in the binary adsorption system, the adsorption rate of Cd(II), evaluated by the calculation of h and k_L parameters, was more rapid than Cu(II), whereas the maximum uptake was found to the more important for Cu(II). Figure 2b shows the importance decrease in the adsorbent amount of each species in mixture as compared to that in single solutions. Despite that Cd(II) was more adsorbed onto COSAC in single solutions ($q_{e,Cd} = 0.141$ mmol/g > $q_{e,Cu} = 0.091$ mmol/g), in binary systems Cd(II) show very low adsorption compared to Cu(II) ($q_{e,Cd(Cd–Cu)} = 0.048$ mmol/g < $q_{e,Cu(Cd–Cu)} = 0.077$ mmol/g).

Compared to single adsorption components, in binary systems, the individual adsorption of Cd(II) and Ni(II) shows an increase in kinetic rates and important decreases in adsorbed amounts with the domination of Cd(II) in binary systems (Fig. 2c). In the presence of cadmium, nickel exhibits a slight drop after 20 min. Measured kinetic rates are in the following trend: $h_{Cd(Cd–Ni)} = 1.380$ mmol/g min > $h_{Ni(Cd–Ni)} = -1.350$ mmol/g min. The examination of

Table 2 The pseudo-second-order kinetic model parameters for single and binary adsorption systems onto COSAC

Metal	$q_{e,exp}$ (mmol/g)	$q_{e.tot,exp}$ (mmol/g)	Pseudo-second-order				
			k_2 (g/mmol min)	$10^2 \cdot h$ (mmol/g min)	$q_{e.cal}$ (mmol/g)	R^2	$10^8 \cdot k_L$ (cm/s)
Ni	0.076	–	2.339	1.39	0.077	0.999	6.346
Cu	0.091	–	1.928	1.67	0.093	0.999	5.715
Cd	0.141	–	1.028	2.13	0.144	0.999	8.818
Cu(Cu–Ni)	0.093	0.169	2.486	2.150	0.093	0.999	8.494
Ni(Cu–Ni)	0.076		2.154	1.240	0.076	0.998	6.416
Cd(Cd–Cu)	0.048	0.125	5.897	1.358	0.048	0.997	4.113
Cu(Cd–Cu)	0.077		1.401	0.830	0.077	0.997	2.932
Cd(Cd–Ni)	0.032	0.050	12.705	1.380	0.033	0.998	5.340
Ni(Cd–Ni)	0.018		−37.47	−1.350	0.019	0.998	−5.264

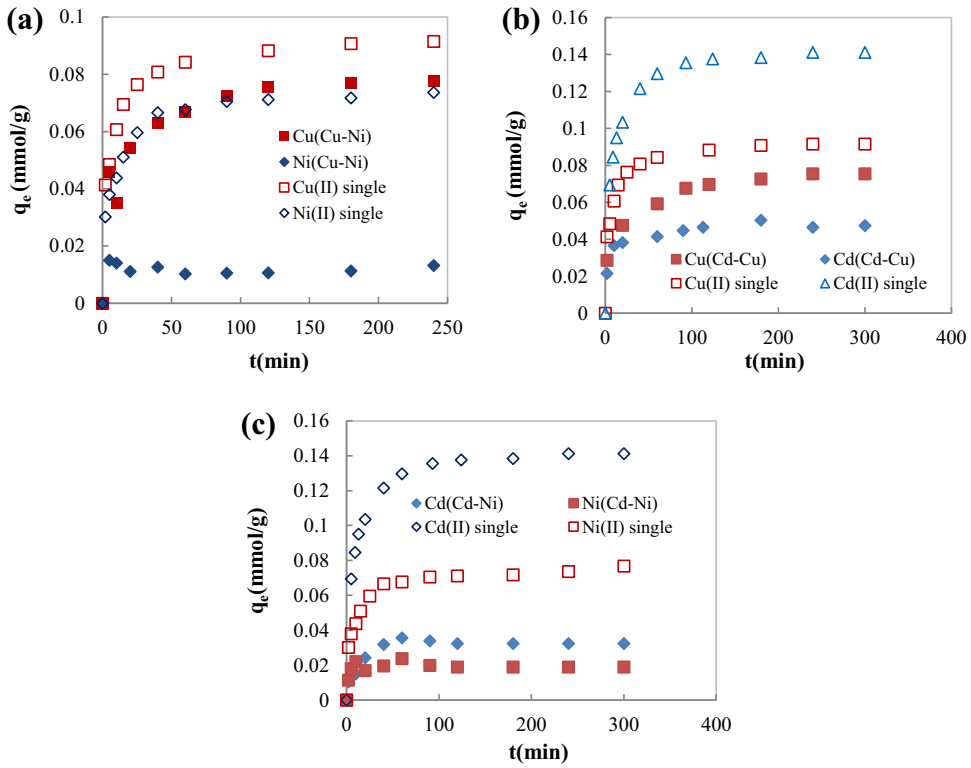

Fig. 2 Single and binary adsorption of **a** Cu(II) and Ni(II); **b** Cu(II)–Cd(II), and **c** Ni(II) and Cd((II) onto COSAC (T: 30 °C; pH: 5; C_0: 1.0 mmol/l; τ_{CA}: 6 g/l; dp: 0.375 mm)

maximum adsorption amounts determined for each metal ions in single and binary systems show that Cd(II) was the most adsorbed one and the following affinity order was observed Cd(II) > Ni(II).

Total experimental adsorbed amount ($q_{e.tot,exp}$(mmol/g)) of both metal ions formed each binary system was calculated (Table 2). The effect between ions in each binary system should be determined (an enhancing or an inhibitor).

As mentioned in Fig. 3, the pseudo-second-order kinetic model fitted the experimental data of binary adsorption systems very well, which can be proved by the good correlation coefficient values and equality between experimental and calculated maximum adsorption amounts (Table 2). The k_L (cm/s) of Cu in the binary system (Cu–Ni) (8.494) is higher than k_L of the single Cu (5.715). Similar to single metal ion adsorption, in mixture solutions with equimolar initial metal ion concentrations 1:1 and base on the adsorption rate h(mmol/g.min) the kinetic adsorption order follow the trend: Cd(II) > Cu(II) > Ni(II).

Equilibrium adsorption isotherms of monosolute systems

Experimental adsorption equilibrium data of Cu(II), Ni(II), and Cd(II) ions are shown in Fig. 4. As can be seen, the obtained isotherms are of L-type or Langmuir type (Giles et al. 1974). Obtained experimental isotherms were evaluated using the commonly used equilibrium models: Freundlich (Eq. (4)), Langmuir (Eq. (5)) and Sips (Eq. (7)) models.

The Freundlich isotherm is an empirical model based on the assumption that adsorption surface are heterogeneous with a non-uniform distribution of heat of adsorption over the surface. The Freundlich equation is given as follows:

$$q_e = K_F C_e^{\frac{1}{n}}, \quad (4)$$

where, K_F ((mmol/g)·(L/mmol)$^{1/n}$) and n are Freundlich parameters, K_F is the constant represents the affinity of the solute for the adsorbent whereas the constant 'n' represents the capacitance of the adsorbent.

The Langmuir isotherm, the monolayer model, was developed to represent chemisorption (Wang 2009). The Langmuir model is based on assumptions that the binding sites are homogeneously distributed over the adsorbent surface, no interaction between adsorbed molecules, and all the binding sites have the same affinity for adsorption of a single molecular layer. The Langmuir model is given by Eq. (5):

$$q_e = \frac{q_{max} K_L C_e}{1 + K_L C_e}, \quad (5)$$

where, q_e (mmol/g), and C_e (mmol/l) are the adsorbed amount of solute and solute concentration at equilibrium time, respectively. The affinity constant K_L (L/mmol) corresponds to the energy constant and describes the

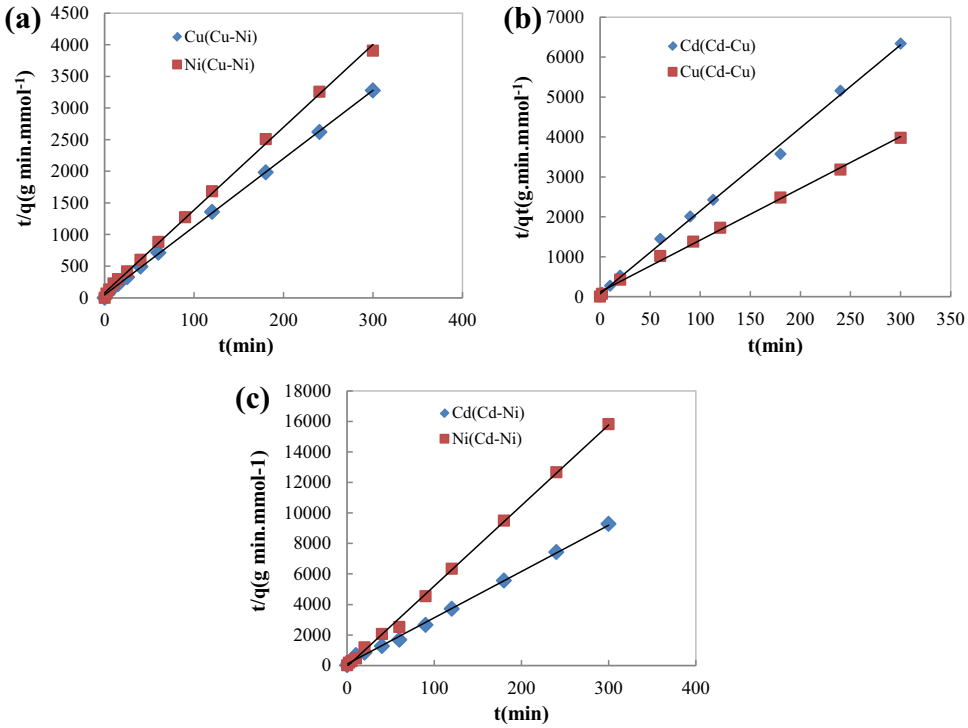

Fig. 3 Pseudo-second-order kinetic model fitting on its linear form to the experimental data **a** Cu(II)–Ni(II), **b** Cu(II)–Cd(II), and **c** Cd(II)–Ni(II) binary adsorption systems (T: 30 °C; pH: 5; C_0: 1.0 mmol/l; τ_{CA}: 6 g/l; dp: 0.375 mm)

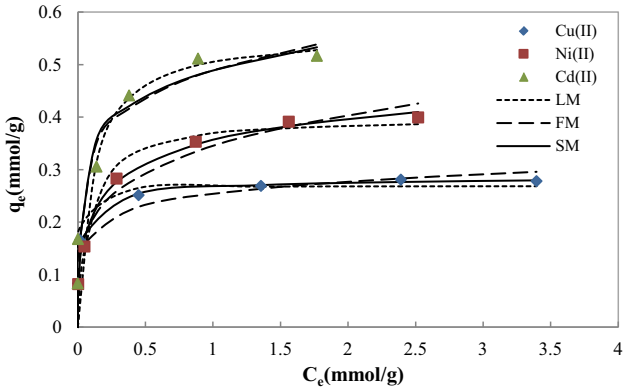

Fig. 4 Adsorption isotherms of Cu(II), Ni(II), and Cd(II) onto COSAC

affinity of the solute for the adsorbent, while q_{max} (mmol/g) corresponds to the monolayer adsorption capacity of the adsorbent.

The essential characteristic of the Langmuir isotherm can be described by a separation factor, which is called the equilibrium constant, R_L, defined as:

$$R_L = \frac{1}{1 + K_L}\frac{1}{C_0}. \quad (6)$$

The adsorption process is favorable for $0 < R_L < 1$ (Chiban et al. 2011).

C_0 is the initial concentration of the adsorbate (mmol/l).

The Sips isotherm is a combination of the Langmuir and Freundlich isotherms. The model equation is similar in form to the Freundlich equation, but it has an asymptotic limit when the concentration is sufficiently high (Al-Asheh et al. 2000):

$$q_e = \frac{q_{ms} \times K_s \times C_e^{ms}}{1 + K_s \times C_e^{ms}}, \quad (7)$$

where q_{ms} (mmol/g) is the maximum adsorption capacity determined by Sips model, K_s (L/mmol)^{ms} is the Sips equilibrium constant and m_s is the Sips model exponent.

The three non-linear models parameters were determined by using Solver program in Microsoft Excel.

In Fig. 4, Langmuir, Freundlich, and Sips nonlinear isotherms are superimposed to the experimental Cu(II), Ni(II), and Cd(II) adsorption data. The corresponding parameters of the models and correlation coefficients are reported in Table 3. The three models predicted quite adequate adsorption equilibrium of the studied metal ions, although the Sips model provided the highest correlation coefficients, which ranged from 0.983 to 0.999.

Points represent the experimental data and lines represent modeling results by the Langmuir model (LM), Freundlich model (FM), and sips model(SM) (pH 5, equilibrium time 10 h, temperature 30 °C).

As seen in Table 3, the value of the theoretical maximum adsorption capacity (mmol/g) determined by the models was found to increase in the order Cu(II) < Ni(II) < Cd(II). The R_L parameter values are lesser than 1, indicating favorable and weakly reversible adsorption of

Table 3 Isotherm constants for the adsorption of Cu(II), Ni(II), and Cd(II) onto COSAC from single solutions (pH 5, equilibrium time 10 h, temperature 30 °C)

Isotherms	Parameters	Heavy metal ions		
		Cu(II)	Ni(II)	Cd(II)
Langmuir	$q_{e.exp}$ (mmol/g)	0.278	0.400	0.516
	q_{ml} (mg/g)	17.080	23.460	62.911
	q_{ml} (mmol/g)	0.278	0.339	0.559
	K_L (L/mmol)	16.077	11.844	25.662
	R_L	0.004	0.056	0.067
	R^2	0.974	0.990	0.981
	SSR	3.76×10^{-4}	9.0×10^{-4}	5.76×10^{-3}
Freundlich	n	7.920	4.364	5.958
	K_F (mmol/l) $(L/g)^{(1/n)}$	0.253	0.344	0.489
	q_{mF} (mmol/g)	0.268	0.386	0.527
	R^2	0.971	0.987	0.983
	SSR	3.64×10^{-3}	3.20×10^{-4}	9.0×10^{-4}
Sips	q_{ms} (mmol/g)	0.298	0.588	2.093
	K_s (L^m/mmol)	8.449	1.530	0.305
	ms	0.467	0.437	0.198
	R^2	0.999	0.996	0.983
	SSR	6.63×10^{-6}	1.20×10^{-4}	9.30×10^{-4}

studied metal ions onto COSAC. The n_F values determined by Freundlich equation were higher than 1.0, indicating heterogeneous adsorption of metal ions onto COSAC.

The differences between maximum capacities of the studied metal ions presented in Table 3 will be discussed knowing that the affinity of the adsorbent for metal ions is usually related to the physicochemical properties of the metal species. The physicochemical properties of the studied heavy metals retrieved from literature are presented in Table 4.

Hossain et al. (2014) interpreted from their adsorption study by using cabbage waste that higher molecular weighted metals are removed in a greater deal than lower molecular weighted metals. In our work, obtained results show that Cd(II) ions with the highest molecular weight (112.4 g/mol) were more adsorbed than the other two metal ions with lower molecular weights Cu(II) (63.556 g/mol) and Ni(II) (58.700 g/mol). As seen in Table 3, the maximum amount of the studied metal adsorbed onto COSAC does not follow the trend to increase with the increase of the metal ion molecular weight.

Table 4 Heavy metals properties (Gao et al. 2009; Minceva et al. 2008; Lima et al. 2007)

	Ni(II)	Cu(II)	Cd(II)
Molecular weight (g/mol)	58.700	63.556	112.4
Ionic radius (A°)	0.69	0.73	0.95
Hydrated ionic radius (A°)	4.04	4.19	4.26
Hydration energy (kJ/mol)	−2105	−2100	−1807
Electro-negativity (Pauling)	1.91	1.90	1.69
Ionization energy (eV)	18.168	20.292	16.908
Polarizability (10^{-24} cm^3)	6.80	6.10	7.36

Cations with small ionic radius are expected to transfer more rapidly to adsorption sites while cations with large ionic radius can cause a quick saturation of the adsorbent due to steric effects resulting in a lower adsorption on the adsorbent surface (Gao et al. 2009). In this study, the opposite trend was found, since adsorption capacity increased with the increase of ionic radius.

Concerning ion hydration for a given valence, small ions have higher charge density than large ions, so they attract more water molecules, resulting in a large hydrated radius. Therefore, the ion with the higher hydrated radius exerts weaker forces of attraction and has more difficulties to reach adsorption sites. When looking at adsorption results obtained in this work (Table 3), the opposite trend is observed.

Similar observation must be stated when discussing hydration energy values. The lower the hydration energy of the ion (in absolute values), the greater the affinity between the ion and functional group of CA (Gao et al. 2009; Minceva et al. 2008); and again the opposite trend was shown. Electronegativity values shown in Table 4 cannot explain the order of affinity for metal ions shown by COSAC, as it has been reported that metals with higher electro-negativity show higher adsorption yields (Li et al. 2003; Lima et al. 2007). Based on the hard soft acid–base (HSAB) theory or Pearson acid-base concept (Auboiroux et al. 1998; Padilla-Ortega et al. 2013), Cu(II) and Ni(II)

are classified as borderline Lewis acid (intermediate properties hard and soft) that can react with hard and soft bases, and Cd(II) as soft Lewis acid that can react with only hard Lewis bases. In aqueous solution, COSAC surface possesses more hard Lewis bases (OH^-, COO^-, CO^-, PO_4^{3-}) than soft Lewis bases. According to this, Cu(II) and Ni(II) should be more adsorbed onto the adsorbent than Cd(II), but again, this reasoning is not consistent with the obtained results.

For all the above considerations, it is evident that the affinity order Cd(II) > Ni(II) > Cu(II) found in this work for the studied metal ions cannot be related to the physicochemical properties of metal cations. Physicochemical properties of metal ions coupled with the steric effects of the adsorbent and physicochemical properties of its surface open the way to a multitude of interpretations that can be contradictory or even confusing. All this discussion reveals, the complexity of the adsorption process of metal cations on the microporous CA that presumably involves several mechanisms related to the different characteristics of both adsorbate and adsorbent. Indeed, different adsorption affinity orders were detected for the same target metal ions by other authors using different kinds of ACs (Table 5). As seen in this table, Kobya et al. (2005) reported the same affinity order than the found in this work when using activated carbon based on apricot stone. Some publications found that adsorption of Cu(II) was preferred to any of the other two metals. Compared to the adsorption capacities of the ACs the four studied heavy metals from single aqueous systems, COSAC is relatively effective adsorbent for the treatment of waste water contaminated with heavy metals.

Equilibrium adsorption isotherms of binary systems

Competitive equilibrium adsorption isotherms of copper, nickel, and cadmium in Cu(II)–Ni(II), Cu(II)–Cd(II), and Ni(II)–Cd(II) binary mixtures are presented in Figs. 5, 7 and 9, respectively. The shapes of measured isotherms in binary systems deviate from Langmuir type, as detected in single systems, to others forms as the concentration of the interfering metal increases. Adsorption experimental values are presented in Table 6.

Cu(II)–Ni(II) binary systems

The plot of the experimental adsorption isotherms of copper and nickel in Cu(II)–Ni(II) binary systems is depicted in Fig. 5. A first glance at this figure suggests that the presence of increasing concentrations of Ni(II) results in an increase of Cu(II) loading capacity (Fig. 5a) while increasing concentrations of Cu(II) exerts the contrary effect and leads to lower Ni(II) adsorption yields when in binary mixtures (Fig. 5b). The effect of nickel on copper adsorption can be clearly shown in Fig. 6a, where the experimental maximum amount of copper adsorbed taken from the obtained copper isotherms in binary mixtures is plotted as a function of nickel initial concentration in the mixtures. The maximum favoring effect of nickel on copper adsorption can be observed for nickel initial concentrations in the range between 0 and 3.0 mmol/l where maximum copper adsorption progressively increased with the increase of nickel initial concentration. Higher nickel initial concentrations provoked only a slight increase of copper adsorption, reaching a maximum value of almost double the maximum capacity found in single solution. Villaescusa et al. (2004) also reported a favoring effect of nickel on copper adsorption when studying the simultaneous adsorption of Cu(II) and Ni(II) onto grape stalks.

The inhibitory effect of copper on nickel adsorption is evidenced by the plot in Fig. 6b. Maximum nickel adsorption dramatically decreased when copper initial concentration increased from 0 to 5.0 mmol/g. The influence of the initial concentration of interfering metal ions on target one forming Cu(II)–Ni(II) binary mixture was also observed by Gao et al.(2009) using oxidized carbon

Table 5 Adsorption order of studied heavy metals using different adsorbents

Adsorbent	Adsorption order	Adsorption capacity (mg/g)	References
Apricot stone AC	Cd(II) > Ni(II) > Cu(II)	33.570–26.080–24.080	Kobya et al. (2005)
Bamboo AC	Cu(II) > Ni(II) > Cd(II)	7.371–6.457–5.170	Liu et al. (2005)
Immobilized tannic acid AC	Cu(II) > Cd(II)	2.224–1.461	Ucer et al. (2006)
Hazelnut hush AC	Cu(II)	6.645	Imamoglu and Tekir (2008)
ACM	Cu(II) > Ni(II)	5.715–2.876	Salido et al. (2009)
ACM-2	Cu(II) > Ni(II)	12.760–7.454	Salido et al. (2009)
Mosobomboo AC (S1C1)	Cu(II) > Cd(II)	0.401–0.174	Lo et al. (2012)
Ma bomboo AC (S1M1)	Cu(II) > Cd(II)	0.400–0.257	Lo et al. (2012)
Potato residue AC	Cu(II) > Ni(II)	26.800–10.000	Luo et al. (2015)
Olive stone AC (COSAC)	Cd(II) > Ni(II) > Cu(II)	62.911–23.460–17.080	This work

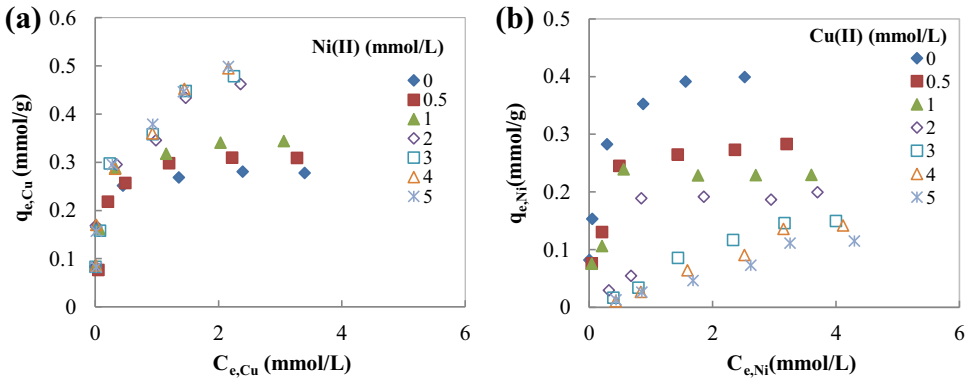

Fig. 5 Adsorption isotherms of **a** Cu(II) in the presence of increasing initial concentration of Ni(II) and **b** of Ni(II) in the presence of increasing concentration of Cu(II) (pH: 5; t_{eq}: 10 h; T: 30 °C; dp: 0.375 mm)

nanotubes as adsorbent. Escudero et al. (2013) found that Cu(II) and Ni(II) were first simultaneously sorbed onto grape stalks wastes but when the active sites started to be scarce the sorbed nickel ions were displaced by copper ions out of the column.

Cu(II)–Cd(II) binary systems

The effect of interactions between Cu(II) and Cd(II) in binary mixtures on the adsorption of both metals onto COSAC can be seen in Fig. 7. The experimental adsorption isotherms of copper in binary systems with cadmium (Fig. 7a) show that the presence of cadmium leads to higher copper adsorption yields as compared to the one shown in single solution. Unlike the results found in the case of Cu(II)–Ni(II) binary mixtures set, copper adsorption was not higher as higher was the initial concentration of cadmium in Cu(II)–Cd(II)binary mixtures. As observed in Fig. 8a, where the plot represents the maximum copper uptake determined at different initial concentrations of cadmium, the highest adsorbed amount of Cu(II) was obtained when cadmium initial concentration in the mixture was 1.0 mmol/l. This maximum value is more than two times the maximum amount of copper uptake in single solution. Up to this cadmium initial concentration, the maximum uptake of copper slightly decreased but it was still higher than that obtained in copper single solution.

Experimental adsorption isotherms of cadmium in the presence of different initial concentrations of copper are presented in Fig. 7b. As observed in this figure, cadmium adsorption is, in general, inhibited by the presence of copper, resulting in values of equilibrium data lower than the ones found when in single solution. Nevertheless, an initial copper concentration of 1.0 mmol/l exhibited a positive effect on Cd(II) adsorption onto COSAC surface and Cd(II) maximum uptake was slightly higher than the value obtained in single solution (8.52% of enhancement) (Fig. 8b). The lowest maximum adsorption data were found for the binary mixture containing 4.0 mmol/l initial cadmium concentrations. It must be remarked that variation of the amount of copper adsorbed as a function of initial concentration of cadmium did not show any clear trend.

Ni(II)–Cd(II) binary systems

The adsorption behavior of Ni(II) in the presence of Cd(II) and of Cd(II) in the presence of Ni(II) can be observed in Fig. 9. As seen in Fig. 9a, the presence of small concentrations of Cd(II) (0.5 mmol/l) caused an increase of Ni(II) adsorption onto COSAC surface. Initial cadmium concentrations higher than this value produced a marked decrease of nickel adsorption equilibrium data as compared to adsorption equilibrium data of nickel in single solution. These results suggest that both favoring and inhibiting effects appear according to the concentration of Cd(II) in solution. This can be clearly seen in Fig. 10 where the maximum amount of Ni(II) adsorbed onto COSAC in single and binary mixtures Ni(II)–Cd(II) is compared. Values of q_{max} vary with the variation of initial concentration of cadmium in the binary mixture without following any trend.

The influence of interfering metal initial concentration on Cd(II) adsorption can also be observed in Fig. 9b, where Cd(II) isotherms in the presence of different initial concentrations of Ni(II) are plotted. The presence of 0.5 mmol/l Ni(II) initial concentration favored cadmium adsorption. Conversely, Ni(II) initial concentrations up to 0.5 mmol/l resulted in a drop of Cd(II) adsorption equilibrium data. The inhibitory effect of Ni(II) on Cd(II) adsorption appeared to be more important than that of Cd(II) on Ni(II) adsorption. As can be observed in Fig. 10a, when Cd(II) initial concentration increased from 0.5 to 2.0 mmol/l, Ni(II) maximum adsorption decreased by about 15%, while for the same interval of variation of nickel concentration in Ni(II)–Cd(II) binary mixtures Cd(II) maximum adsorption decreased by around 68% (Fig. 10b). From the foregoing results, it can be concluded that Ni(II) exhibited greater inhibitory effect on Cd(II) adsorption during the

Table 6 Metal sorption experimental values in single and binary mixtures (pH 5, equilibrium time 10 h, temperature 30 °C)

C_0 (mmol/l) of interfering metal ion	$q_{max,i}^{single}$ (mmol/g)	$q_{max,i}^{binary}$ (mmol/g)	$q_{max,j}^{binary}$ (mmol/g)	$q_{max,tot} = q_{max,i}^{binary} + q_{max,j}^{binary}$ (mmol/g)	$q_{max,i}^{binary}/q_{max,i}^{single}$
Cu(Cu–Ni)					
0.5	0.278	0.309	0.013	0.322	1.111
1		0.344	0.015	0.359	1.237
2		0.462	0.046	0.508	1.661
3		0.478	0.074	0.552	1.719
4		0.499	0.107	0.606	1.795
5		0.499	0.089	0.588	1.795
Ni(Ni–Cu)					
0.5	0.399	0.283	0.083	0.366	0.707
1		0.230	0.157	0.387	0.575
2		0.200	0.295	0.495	0.500
3		0.150	0.378	0.528	0.375
4		0.142	0.446	0.588	0.355
5		0.115	0.499	0.614	0.287
Cu(Cu–Cd)					
0.5	0.278	0.510	0.030	0.540	1.834
1		0.503	0.065	0.568	1.809
2		0.472	0.191	0.663	1.697
3		0.476	0.098	0.574	1.712
4		0.528	0.551	1.079	1.899
5		0.493	0.493	0.986	1.773
Cd(Cd–Cu)					
0.5	0.516	0.331	0.075	0.406	0.641
1		0.560	0.158	0.718	1.085
2		0.374	0.472	0.846	0.724
3		0.331	0.415	0.746	0.641
4		0.166	0.423	0.589	0.321
5		0.309	0.493	0.802	0.598
Ni(Ni–Cd)					
0.5	0.399	0.417	0.064	0.481	1.042
1		0.376	0.088	0.464	0.940
2		0.284	0.192	0.476	0.710
3		0.296	0.299	0.595	0.740
4		0.308	0.420	0.728	0.770
5		0.290	0.488	0.778	0.725
Cd(Cd–Ni)					
0.5	0.516	0.596	0.053	0.649	1.155
1		0.498	0.108	0.606	0.965
2		0.507	0.199	0.706	0.982
3		0.551	0.302	0.853	1.067
4		0.416	0.282	0.698	0.806
5		0.457	0.348	0.805	0.885

i target metal ion, *j* interfering metal ion

competitive adsorption. This indicates the displacement effect of Ni(II) to adsorbed Cd(II) ions and to bind itself the empty adsorbent adsorption sites. Srivastava et al. (2009) explain the important adsorbed amount on rice hush ash (RHA) of Ni(II) than that of Cd(II) by the fact that there are possible interactions effects between different species in

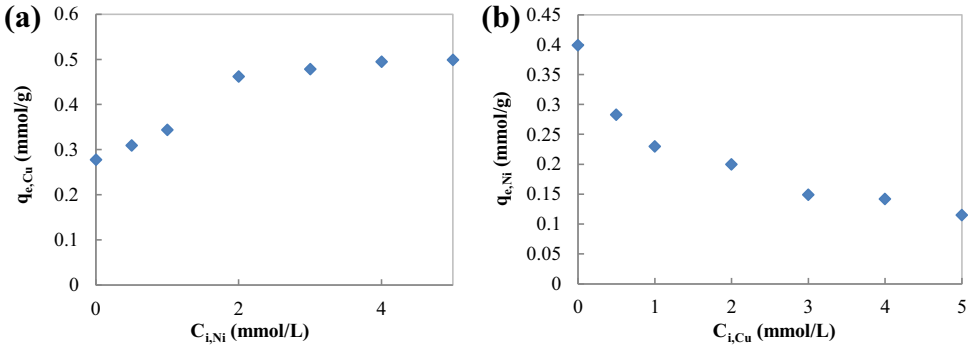

Fig. 6 Effect of initial concentration of interfering metal in maximum adsorption of target metal. **a** Target metal Cu (II) interfering metal Ni(II). **b** Target metal Ni(II) interfering metal Cu(II) (pH: 5; t_{eq}: 10 h; T: 30 °C; dp: 0.375 mm)

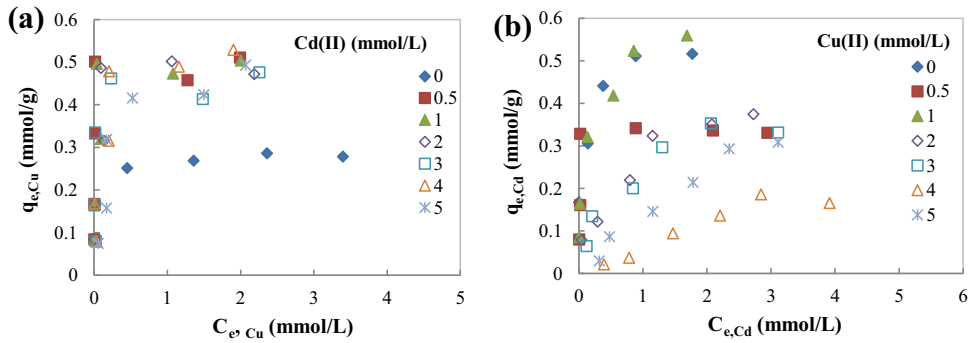

Fig. 7 Adsorption isotherms of **a** Cu(II) in the presence of increasing initial concentration of Cd(II) and **b** Cd(II) in the presence of increasing initial concentration of Cu(II) (pH: 5; t_{eq}: 10 h; T: 30 °C; dp: 0.375 mm)

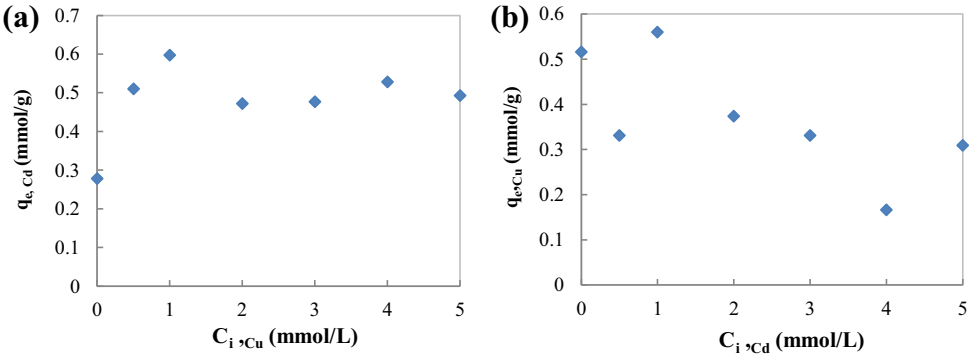

Fig. 8 Effect of initial concentration of interfering metal in maximum adsorption of target metal. **a** Target metal Cu (II) interfering metal Cd(II), **b** target metal Cd(II) interfering metal Cu(II) (pH: 5; t_{eq}: 10 h; T: 30 °C; dp: 0.375 mm)

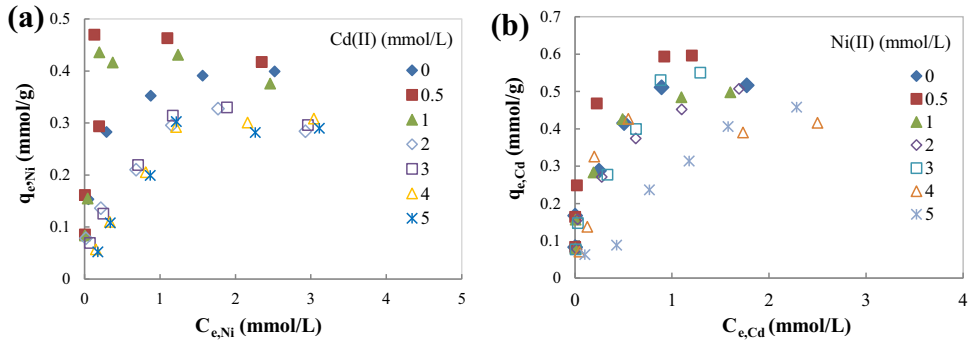

Fig. 9 Adsorption isotherms of **a** Ni(II) in the presence of increasing initial concentration of Cd(II) and **b** Cd(II) in the presence of increasing initial concentration of Ni(II) (pH: 5; t_{eq}: 10 h; T: 30 °C; dp: 0.375 mm)

solution and in particular potential interaction on the surface depending on the adsorption mechanism. The foregoing results show that the type of interactions between the two metals in a mixture depends on the initial concentration of the interfering metal, resulting in different adsorption yields of both components of the mixture.

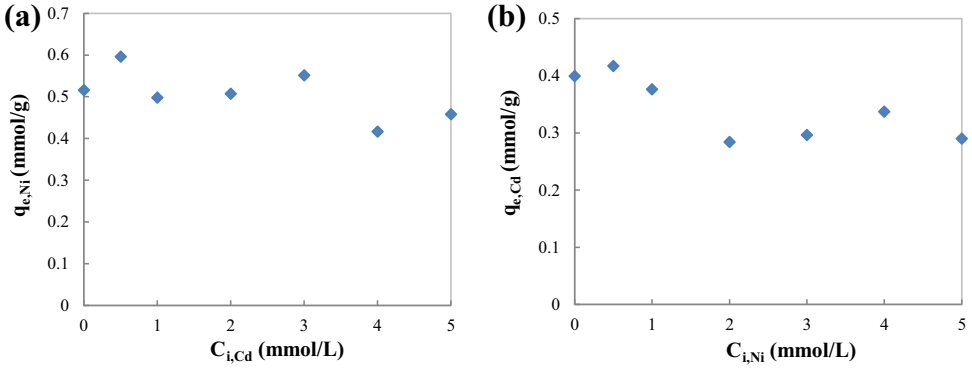

Fig. 10 Effect of initial concentration of interfering metal in maximum adsorption of target metal. **a** Target metal Ni(II) interfering metal Cd(II) and **b** target metal Cd(II) interfering metal Ni(II) (pH: 5; t_{eq}: 10 h; T: 30 °C; dp: 0.375 mm)

Discussion

Table 6 summarizes the experimental adsorption values obtained for the studied metals both in single ($q_{max,i}^{single}$) and binary mixture ($q_{max,i}^{binary}$) the total amount of metal ions adsorbed ($q_{max,tot}$) and the ratio between metal maximum adsorption in single solution and in binary mixture ($q_{max,i}^{binary}/q_{max,i}^{single}$).

As seen in Table 6, adsorption of copper is always favored by the presence of both nickel and cadmium, which indicates an enhancement effect. The amount of copper adsorbed increased from 0.278 mmol/g, its maximum adsorption in single solution, to around 0.500 mmol/g with the increase of nickel and cadmium initial concentrations from 0 to 5 mmol/l, respectively. A similar amount of maximum copper adsorbed was also attained in the cadmium and nickel isotherms when copper initial concentration was 5.0 mmol/l. The maximum amount of cadmium and nickel in their respective sets of isotherms in binary mixtures with copper show how the uptake of these two metals is negatively affected by an increase in the concentration of copper. These two metal ions when in binary mixtures with copper were not able to reach the maximum adsorption found in single solutions. On its turn, 5.0 mmol/l initial concentration of copper reached a maximum adsorption of around 0.500 mmol/g with independence, whether it is in single or in binary mixture.

Results corresponding to maximum experimental adsorption values of cadmium and nickel when in binary mixtures reflect that both metals only keep the maximum adsorption determined in single solutions when they are the target metal and the interfering metal initial concentration is 0.5 mmol/l. The competition between these two metals for the adsorbent sites is evident. Nickel adsorption suffers more the effect of the presence of cadmium than the inverse. When the initial concentration of the interfering metal is 5.0 mmol/l, loss of maximum adsorption with respect to the one determined in single solution is 27.5 and 11.43% for nickel and cadmium, respectively. Others works found that cadmium adsorption decreased with the increase of nickel (Padilla-Ortega et al. 2013; Srivastava et al. 2009).

Adsorption results of the studied metals in binary mixtures reveal a new metals affinity order Cu(II) > Cd(II) > Ni(II). Gwenzi et al. (2014) also found that the affinity order Cd(II) > Cu(II) found in mono solute solutions changed to Cu(II) > Cd(II) when the metals were forming binary mixtures. As seen in Table 6, the sum of the maximum adsorption values of both metals in binary mixtures ($q_{max,tot}$) is in most of the cases less than the sum of those in single solutions indicating that the joined effect on each other metal is antagonistic. Antagonistic effects were also reported in the literature (Hossain et al. 2014; Srivastava et al. 2009). Conversely, a synergistic effect was observed in the case of Cu(II)–Cd(II) isotherms when cadmium initial concentration were 4.0 and 5.0 mmol/l. Synergistic effects were also reported by Luo et al. (2015) for heavy metal adsorption onto activated carbon.

Moreover, values of $q_{max,tot}$ fluctuate without following any clear trend with the increase of the interfering metal. This fluctuation indicates the great importance of the initial concentration of the interfering metal metals as it is responsible for the synergistic and antagonistic effects observed in the present study.

The last column in Table 6 corresponds to the ratio between the maximum amount of target metal adsorbed in single solution and in binary mixtures. Ratios higher than unity indicate that the presence of a second metal enhances adsorption of the target metal (i), ratios equal to unity no effect on adsorption of the interfering metal and lower than unity inhibitory effect on target metal adsorption (Mohan and Singh 2002).

Ratios corresponding to copper are always higher than unit, increase with the increase of interfering metal concentration and range between 1.111 and 1.795 and 1.697 and 1.899 when the interfering metal is nickel and cadmium, respectively. The explanation of higher maximum adsorption yields of a metal when in binary mixture must be attributed to the increase of ionic strength of the solution

due to the second metal that provides of driving force to reach less accessible active sites. It is remarkable that the copper adsorption ratio $q_{max,i}^{binary}/q_{max,i}^{single}$ increases with the increase of nickel but copper adsorption ratio does not follow any trend when the interfering metal is cadmium. Nickel adsorption ratios lower than unit show that nickel adsorption is suppressed by the presence of the interfering metal. The values of the nickel adsorption ratios decrease from 0.707 to 0.287 (59%) when increasing the concentration of copper but they don't follow any trend when the interfering metal was cadmium. Moreover, the nickel adsorption ratio was 1.042 when initial cadmium concentration was 0.5 mmol/l. The most clear evidence that adsorption of both metals in the binary mixture depend on metals concentration is found in the adsorption ratio values of cadmium corresponding to the binary mixtures Cd(II)–Cu(II) and Cd(II)–Ni(II). Cadmium adsorption ratios were lower than unity and their value varied with the initial concentration of copper or nickel without any trend with respect to initial concentration of the interfering metal. Note that in the case of Cd(II)–Ni(II), binary mixture cadmium adsorption ratios are around unity. Values around unity mean that both metals exert little enhancing or suppressing effects on each other's adsorption. In the case of Cd(II)–Cu(II), binary mixture cadmium adsorption ratios only slightly exceeded unity when the initial concentration was 0.5 mmol/l and the rest of the values were far from unity confirming the inhibitory effect of copper on cadmium adsorption.

Conclusions

An activated carbon (COSAC) prepared from low-cost olive stone agriculture by-product was used as adsorbent for Cd(II), Ni(II), and Cu(II) in single and binary solutions. From the obtained results, the following conclusions can be retrieved:

- COSAC shows a significant capacity to remove the studied metal ions from single solution and binary mixtures. In single metal solutions, maximum capacity of studied metals was found to decrease in the order: Cd(II) > Ni(II) > Cu(II) while a change of this trend was observed in binary mixtures where Cu(II) > Cd(II) > Ni(II).
- In binary systems, maximum capacity of COSAC for each of the metals resulted influenced by the presence of a second metal. In most of the binary systems, the net interactive effect between the metals forming the mixtures was found to be antagonistic, as the total amount of metal adsorbed was less than the sum of individual maximum capacity found in single metal solutions. However, a synergistic effect was observed in the case of Cu(II)–Cd(II) at high initial concentrations. Cu(II) adsorption in binary mixtures was always higher than in single solution.
- In Cd(II)–Ni(II) and Ni(II)–Cd(II) binary systems, 0.5 mmol/l initial concentration of interfering metal ion was favorable for target ion adsorption. Higher concentrations resulted in inhibitory effects on each other metal adsorption. The extent of these effects was found to be dependent on the initial concentration of the interfering metal.

Finally, this work highlights the important influence of the initial concentration of the interfering metal on mutual metal interactions that result in both inhibitory and enhancing effects on metal adsorptions. This work opens the way for further research to better understand the exact adsorption mechanism of heavy metal adsorption onto COSAC from multicomponent real systems.

Acknowledgements The authors wish to acknowledge the University of Gabes, Tunisia, for the financial support and MiMa Laboratory, Department d'Enginyeria Quimica, Agrariai Tecnologia Agroalimentaria, Universitat de Girona for its contribution to this work.

Compliance with ethical standards

Conflict of interest All of the authors have declared no conflicts of interest.

References

Abbas ST, Mustafa M, Al-Faize AZ, Rah AZ (2013) Adsorption of Pb^{2+} and Zn^{2+} ion from oil wells onto activated carbon produced from Rice Husk in batch adsorption process. J Chem Pharm Res 4:240–250

Ahmad A, Ghufran R, Raizal WM (2010) Cd(II), Pb(II) and Zn(II) removal from contaminated water by biosorption using activated sludge biomass, CLEAN-soil. Air Water 32:153–158

Al-Asheh S, Banat F, Al-Omari R, Duvnjak Z (2000) Predictions of binary sorption isotherms for the sorption of heavy metals by pine bark using single isotherm data. Chemosphere 41:659–665

Alslaibi TM, Abustan I, Ahmad MA, Abu Foul A (2015) Comparison of activated carbon prepared from olive stones by microwave and conventional heating for iron (II), lead (II), and copper (II) removal from synthetic wastewater. AIChE 33:1074–1084

Amarasinghe BK, Williams RA (2007) Tea waste as a low cost adsorbent for the removal of Cu and Pb from wastewater. Chem Eng J 132:299–309

Anirudhan TS, Sreekumari SS (2011) Adsorptive removal of heavy metal ions from industrial effluents using activated carbon derived from waste coconut buttons. J Environ Sci 23:1989–1998

Auboiroux M, Melou F, Bergaya F, Touray JC (1998) Hard and soft acid-base model applied to bivalent cation selectivity on a 2:1 clay mineral. Clays Clay Miner 46:546–555

Baccar R, Bouzid J, Feki M, Montiel A (2009) Preparation of activated carbon from Tunisian olive-waste cakes and its application for adsorption of heavy metal ions. J Hazard Mater 162:1522–1529

Bailey SE, Olin TJ, Bricka RM, Adrian DD (1999) A review of potentially low cost sorbents for heavy metals. Water Res 33:2469–2479

Bakircioglu Y, Bakircioglu D, Akman S (2003) Solid phase extraction of bismuth and chromium by rice husk. J Trace Microprobe Tech 21:467–478

Bohli T, Ouederni A (2016) Improvement of oxygen-containing functional groups on olive stones activated carbon by ozone and nitric acid for heavy metals removal from aqueous phase. Environ Sci Pollut Res 23:15852–15861

Bohli T, Ouederni A, Fiol N, Villaescusa I (2015) Evaluation of an activated carbon from olive stones used as an adsorbent for heavy metal removal from aqueous phases. CRC 18:88–99

Brasquet CF, Reddad Z, Kadirvelu K, Cloirec P (2002) Modelling the adsorption of metal ions (Cu^{2+}, Ni^{2+} and Pb^{2+}) onto ACCs using surface complexation models. Appl Surf Sci 196:356–365

Ceyhan AA, Sahin O, Baytar O, Saka C (2013) Surface and porous characterization of activated carbon prepared from pyrolysis of biomass by two-stage produce at low activation temperature and it's the adsorption of iodine. J Anal Appl Pyrolysis 104:378–383

Chiban M, Soudani A, Sinan F, Persin M (2011) Single, binary and multi-component adsorption of some anions and heavy metals on environmentally friendly *Carpobrotus edulis* plant. Coll Surf B Biointerfaces 82:267–276

Cui X, Fang S, Yao Y, Li T, Ni Q, Yang X, He Z (2016) Potential mechanisms of cadmium removal from aqueous solution by *Canna indica* derived biochar. Sci Total Environ 562:517–525

Depci T, Kul AR, Onal Y (2012) Competitive adsorption of lead and zinc from aqueous solution on activated carbon prepared from Van apple pulp: study in single- and multi-solute systems. Chem Eng J 200:224

Escudero C, Poch J, Villaescusa I (2013) Modelling of breakthrough curves of single and binary mixtures of Cu(II), Cd(II), Ni(II) and Pb(II) onto grape stalks waste. Chem Eng J 1217:129–138

Fu F, Wang Q (2011) Removal of heavy metal ions from wastewaters: a review. J Environ Manag 92:407–418

Gao Z, Bandosz TJ, Zhao Z, Han M, Qiu J (2009) Investigation of factors affecting adsorption of transition metals on oxidized carbon nanotubes. J Hazard Mater 167:357–365

Gharib H, Ouederni A (2005) Transformation du grignon d'olive Tunisien en charbon actif par voie chimique à l'acide phosphorique. Récents Progrès en Génie des Procédés: Xeme Congrès de la SFGP: le Génie des Procédés Vers de Nouveaux Espaces, Toulouse 2005: Numéro 92

Giles CH, Smith D, Huitson A (1974) A general treatment and classification of the solute adsorption isotherm. I. Theoretical. J Coll Interface Sci 47:755–765

Gwenzi W, Musarurwa T, Nyamugafata P (2014) Adsorption of Zn^{2+} and Ni^{2+} in a binary aqueous solution by biosorbents derived from sawdust and water hyacinth (*Eichhornia crassipes*). Water Sci Technol 70:1419–1427

Hossain MA, Ngo HH, Guo WS, Nghiem LD, Hai FI, Vigneswaran S, Nguyen (2014) Competitive adsorption of metals on cabbage waste from multi-metal solutions. Bioresour Technol 160:79–88

Imamoglu M, Tekir O (2008) Removal of copper (II) and lead (II) ions from aqueous solutions by adsorption on activated carbon from a new precursor hazelnut husks. Desalination 228:108–113

Kasnejad MH, Esfandiari A, Kaghazchi T, Asasian N (2012) Effect of pre-oxidation for introduction of nitrogen containing functional on Cu(II) adsorption. J Taiwan Inst Chem Eng 43:736–740

Knaebel KS (1995) For your next separation consider adsorption. Chem Eng 73:92–102

Kobya M, Demirbas M, Senturk E, Ince M (2005) Adsorption of heavy metal ions from aqueous solutions by activated carbon prepared from apricot stone. Bioresour Technol 96:1518–1521

Laus R, de Favere VT (2011) Competitive adsorption of Cu(II) and Cd(II) ions by chitosan crosslinked with epichlorohydrin-triphosphate. Bioresour Technol 100:8769–8776

Li YH, Ding J, Luan Z, Di Z, Zhu Y, Xu C, Wu D, Wei B (2003) Competitive adsorption of Pb^{2+}, Cu^{2+} and Cd^{2+} ions from aqueous solutions by multiwalled carbon nanotubes. Carbon 41:2787–2792

Lima IM, Marhsall WE, Klasson TK (2007) Removal of heavy metals from solution by a novel swine manure-based activated carbon. USDA ARS Southern Regional Research Center, New Orleans

Liu SX, Chen XY, Chen X, Sun CL (2005) Effect of acid-base two steps surface modification on the adsorption of Cr(VI) onto activated carbon. Environ Sci 26:89–93

Lo SF, Wang SY, Tsai MJ, Lin LD (2012) Adsorption capacity and removal efficiency of heavy metal ions by Moso and Ma bamboo activated carbons. Chem Eng Res Design 90:1397–1406

Luo X, Zhang Z, Zhou P, Liu Y, Maa G, Lei Z (2015) Synergic adsorption of acid blue 80 and heavy metal ions (Cu^{2+}/Ni^{2+}) onto activated carbon and its mechanisms. J Ind Eng Chem 27:164–174

Ma X, Yang ST, Tang H, Liu Y, Wang H (2015) Competitive adsorption of heavy metal ions on carbon nanotubes and the desorption in simulated biofluids. J Coll Inter Sci 448:347–355

Madhava-Raoa M, Rameshb A, Purna Chandra Raoa G, Seshaiaha K (2006) Removal of copper and cadmium from the aqueous solutions by activated carbon derived from *Ceiba pentandra* hulls. J Hazard Mater 129:123–129

Minceva M, Fajgar R, Markovska L, Meshko V (2008) Comparative study of Zn^{2+}, Cd^{2+} and Pb^{2+} removal from water solution using natural clinoptilolitic zeolite and commercial granulated activated carbon. Equilibrium of adsorption. Sep Sci Technol 43:2117–2143

Mohan D, Singh KP (2002) Single-and multi-component adsorption of cadmium and zinc using activated carbon derived from bagasse—an agricultural waste. Water Res 36:2304–2318

Norme Tunisienne NT. 106.002 (1989) Relative aux rejets d'effluents dans le milieu hydrique (Protection de l'environnement)

Padilla-Ortega E, Leyva-Ramos R, Flores-Cano JV (2013) Binary adsorption of heavy metals from aqueous solution onto natural clays. Chem Eng J 225:535–546

Pehlivan E, Yanık BH, Ahmetli G, Pehlivan M (2008) Equilibrium isotherm studies for the uptake of cadmium and lead ions onto sugar beet pulp. Bioresour Technol 99:3520–3527

Porpuri SR, Vijaya Y, Boddu Abburi VMK (2009) Adsorptive removal of copper and nickel ions from water chitosan coated PVC beads. Bioresour Technol 100:194–199

Salido MLG, López-Garzón R, Arranz-Mascarós P, Gutiérrez-Valero MD, Santiago-Medina A, García-Martín J (2009) Study of the adsorption capacity to Co^{2+}, Ni^{2+} and Cu^{2+} ions of an active carbon/functionalized polyamine hybrid material. Polyhedron 28:3781–3787

Singha S, Sarkar U, Luharuka P (2013) Functionalized granular activated carbon and surface complexation with chromates and bi-chromates in wastewater. Sci Total Environ 447:472–487

Slobodan KM, Cerovic LS, Cokesa DM, Zec S (2007) The influence of cationic impurities in silica on its crystallization and point of zero charge. J Coll Inter Sci 309:155–159

Srivastava VC, Mall ID, Mishra IM (2009) Competitive adsorption of cadmium (II) and nickel metal ions from aqueous solution onto rice husk ash. Chem Eng Process Process Intensif 48:370–379

Tsibranska I, Hristova E (2010) Modelling of heavy metal adsorption into activated carbon from apricot stones in fluidized bed. Chem Eng Process 49:1122–1127

Ucer A, Uyanik A, Aygun SF (2006) Adsorption of Cu(II), Cd(II), Zn(II), Mn(II) and Fe(III) ions by tannic acid immobilized activated carbon. Sep Purif Technol 47:113–118

Villaescusa I, Fiol N, Martínez M, Miralles N, Poch J, Serarols J (2004) Removal of copper and nickel ions from aqueous solutions by grape stalks wastes. Water Res 38:992–1002

Wang XS (2009) Equilibrium and kinetic analysis for Cu^{2+} and Ni^{2+} adsorption onto-mordenite. Environ Pollut Toxicol J 1:107–111

WHO (2011) Guidelines for drinking water quality, 4th edn. World Health Organization, Geneva

Wibowo N, Setiyadhi L, Wibowo D, Setiawan J, Ismadji S (2007) Adsorption of benzene and toluene from aqueous solutions onto activated carbon and its acid and heat treated forms: influence of surface chemistry on adsorption. J Hazard Mater 146:237–242

Wong KK, Lee CK, Low KS, Haron MJ (2003) Removal of Cu and Pb by tartaric acid modified rice husk from aqueous solutions. Chemosphere 50:23–28

Zhang B, Xu P, Qiu Y, Yu Q, Ma J, Wu H, Luo G, Xu M, Yao H (2015) Increasing oxygen functional groups of activated carbon with nonthermal plasma to enhance mercury removal efficiency for flue gases. Chem Eng J 263:1–8